Electron distribution function in short-pulse photoionization

B. Hafizi,[1] P. Sprangle,[2] J. R. Peñano,[2] and D. F. Gordon[1]
[1]*Icarus Research, Inc., P.O. Box 30780, Bethesda, Maryland 20824-0780*
[2]*Plasma Physics Division, Naval Research Laboratory, Washington, DC 20375-5346*
(Received 4 February 2003; published 23 May 2003)

Two well-known limiting regimes of photoionization, when a laser beam interacts with a gas, correspond to the tunneling and the multiphoton processes. The latter dominates in the low-intensity regime, while the former is appropriate at higher intensities. Electrons are born with negligible velocity in tunneling ionization, while in l-photon ionization they are born with a fixed energy determined by l, the photon energy and the ionization potential of the molecule. The transport equation for the distribution function of electrons can be integrated along the characteristics defined by the classical equations of motion in the laser field. Expressions for the distribution function have been obtained in the two regimes using the appropriate analytical form for the ionization rate. Results from two-dimensional particle-in-cell simulations and illustrative plots of the distribution function are presented and discussed.

DOI: 10.1103/PhysRevE.67.056407 PACS number(s): 52.25.Jm, 52.20.Dq, 32.80.Fb, 32.80.Rm

I. INTRODUCTION

Ionization of a gas that is subjected to electromagnetic radiation is often analyzed in two well-known limiting cases [1,2]. In the first, free electrons in the gas gain energy from the electric field and ionize the molecules on impact, leading to the release of secondary electrons and avalanche breakdown. The analysis in this paper is limited to ionization by relatively short, intense laser pulses where avalanche breakdown is generally negligible. In the second route, the field is directly responsible for detaching electrons from the atoms or molecules [3–5]. This route, referred to as photoionization, is further subdivided into two regimes, namely, tunneling ionization and multiphoton ionization (MPI). In tunneling ionization the Coulomb barrier is deformed by the electric field of the radiation, allowing a bound-electron wave function to tunnel through and become a propagating wave function. In MPI, on the other hand, an electron jumps from a bound state into the continuum by absorbing a sufficient number of photons. There have been a number of experiments aimed at characterizing the two regimes [6–8]. The differing physical circumstances of these two regimes are expected to lead to different distribution of electrons. The purpose of this paper is to derive analytical forms for the electron distribution function in the two regimes. There are many circumstances where the detailed distribution of photoelectrons is of interest, an example being attosecond spectroscopy [9,10]

The plan of the paper is as follows. In Sec. II the two regimes of photoionization are distinguished, the transport equation is solved, and analytical forms for the electron distribution function are obtained. In Sec. III the distribution functions are numerically evaluated and momentum-space plots are shown to illustrate the different characteristics associated with the two regimes. Two-dimensional particle-in-cell simulation results are also presented to demonstrate an interesting momentum-space pattern that is characteristic of tunneling ionization.

II. PHOTOIONIZATION

In this section the formalism for evaluating the electron distribution function in the two regimes of photoionization is set up. To do so, it is first necessary to have a quantitative measure for distinguishing the two regimes. Next, formulas for the ionization rate in the two regimes are given, the transport equation for the distribution function is written down and formally integrated along the characteristics. Finally the characteristics, i.e., the relativistically correct, classical electron orbits in the laser field are obtained.

A. Tunnel vs multiphoton photoelectric effect and the Keldysh parameter

The ionization energy of a molecule is denoted by U_i. In isolation, a molecule has a set of discrete, bound energy levels. In the presence of an electric field $\mathbf{E}$ the Coulomb potential is deformed and a potential barrier of finite width develops. The width Δ of this barrier is proportional to U_i and inversely proportional to $E \equiv |\mathbf{E}|$; i.e., $\Delta \sim U_i/(|e|E)$, where e is the charge on an electron. Denoting the electronic mass by m, the typical atomic electron velocity is $v \sim (2U_i/m)^{1/2}$, and therefore the transit time of an electron through the barrier is $\tau_{tunnel} \sim \Delta/v \sim (2mU_i)^{1/2}/(|e|E)$. If ω is the frequency of the radiation field, the Keldysh parameter $\gamma_K \equiv \omega \tau_{tunnel}$ is expressible as [11]

$$\gamma_K = \omega \frac{(2mU_i)^{1/2}}{|e|E}. \tag{1}$$

In the quasistatic or high-field limit, $\gamma_K \ll 1$, ionization proceeds by tunneling of electrons through the barrier. In the opposite limit, $\gamma_K \gg 1$, ionization takes place via multiphoton detachment of electrons. The two regimes are sketched in Fig. 1.

Equation (1) may be rewritten to reveal an alternative physical meaning of γ_K. In a linearly polarized oscillatory electric field the average electron oscillation (quiver or pon-

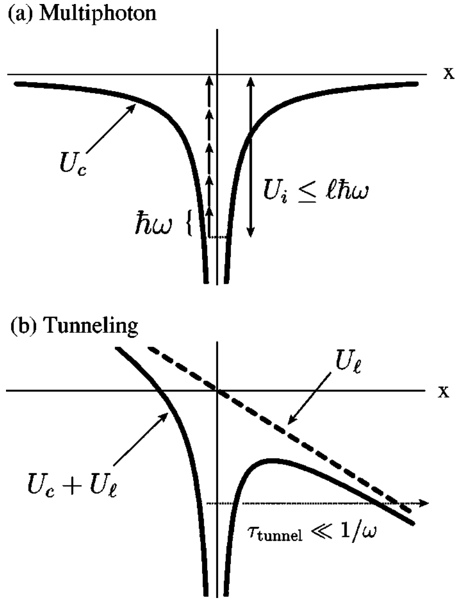

FIG. 1. One-dimensional schematic contrasting two regimes of photoionization. The Coulomb potential is denoted by U_c, the ionization potential of an energy level by U_i, and the potential due to the laser field by U_ℓ. In (a) l or more photons of frequency ω are sufficient to raise a bound electron into the continuum. The "static" sketch shown in (b) is valid provided the tunneling time is short compared to the optical period (i.e., $\tau_{tunnel} \ll 1/\omega$).

deromotive) energy is $U_p = \frac{1}{4}m(|e|E_0/m\omega)^2$. In terms of U_p, $\gamma_K = (U_i/2U_p)^{1/2}$, where E_0 is the amplitude of the electric field. In practical units,

$$\gamma_K = \frac{2.31}{\lambda[\mu\mathrm{m}]}\left[\frac{U_i[\mathrm{eV}]}{I_0\ [\mathrm{TW/cm^2}]}\right]^{1/2},$$

where λ is the wavelength and $I_0 = (cn_0/8\pi)E_0^2 \approx (c/8\pi)E_0^2$ is the average intensity of the electromagnetic field in a rarefied gas with refractive index $n_0 \approx 1$.

B. Ionization rate

Neglecting attachment and recombination the rate equation for electron density n is given by $\partial n/\partial t = Wn_n$, where W is the ionization rate and n_n is the neutral gas density. The instantaneous ionization rate in the tunneling regime W_{tun} may be obtained by employing the $\gamma_K \ll 1$ limit of the general analysis of Keldysh [11–13],

$$W_{tun} = 4\Omega_0\left(\frac{U_i}{U_H}\right)^{5/2}\left(\frac{I_H}{I(t)}\right)^{1/2}\exp\left[-\frac{2}{3}\left(\frac{U_i}{U_H}\right)^{3/2}\left(\frac{I_H}{I(t)}\right)^{1/2}\right], \tag{2}$$

where $I(t) = (c/4\pi)E^2(t)$ is the intensity of the laser beam (assumed to be linearly polarized), $\Omega_0 = 4.1\times10^{16}\ \mathrm{s}^{-1}$ is the fundamental atomic frequency, $I_H = 3.6\times10^{16}\ \mathrm{W/cm^2}$ and $U_H = 13.6$ eV is the ionization energy of hydrogen. The ionization rate in the tunneling regime is a highly sensitive function of the electric field through the exponential factor in Eq. (2). This is a reflection of the exponentially small probability for an electron to tunnel through the Coulomb barrier. Equation (2) is valid provided (i) $\hbar\omega \ll U_i$ (to avoid single-photon ionization) and (ii) $U_p \gg \hbar\omega/(4\gamma_K^3)$ [for validity of the quasiclassical (WKB) solution of Schrödinger's equation]. Here, $\hbar$ is Planck's constant divided by 2π. For extremely intense laser beams, the barrier is completely suppressed and the electronic wave function extends beyond the molecule. This "over the barrier" regime is outside the scope of present analysis [14].

In multiphoton ionization the kinetic energy of an electron is given by an expression that is reminiscent of Einstein's for the photoelectric effect, i.e.,

$$\mathcal{E} = l\hbar\omega - U_i, \tag{3}$$

where l is an integer. In the limit $\gamma_K \gg 1$, Keldysh's analysis leads to an expression for the multiphoton ionization rate W_{MPI} that has an algebraic dependence on the laser electric field; i.e., $W_{MPI} \propto E^{2l}$. In numerical terms, Keldysh's rate is found to disagree significantly with experimental observations. While more sophisticated models exist (e.g., Ref. [15]), for this analysis it is expedient to make use of an empirical relationship that closely resembles observations. In particular,

$$W_{MPI} = \frac{2\pi\omega}{(l-1)!}\left(\frac{I}{I_{MPI}}\right)^l, \tag{4}$$

where $I_{MPI} = \hbar\omega^2/\sigma_{MPI}$ and σ_{MPI} is an empirically-determined cross section. In reference to Eq. (3), it should be remarked that the number of photons absorbed by the molecule can exceed the minimum number required to reach the ionization limit. In this case the electron emerges with additional kinetic energy, determined by the excess photon energy.

C. Transport equation

The transport equation for the distribution function f of electrons is given by $df/dt = S$, where the form of the source term S depends on the process by which electrons are born. Specifically,

$$\frac{df}{dt} = n_n\begin{cases} W_{tun}(E)\,\delta(u), & \text{tunneling} \\ W_{MPI}(E)\,\delta(l\hbar\omega - U_i - (\gamma-1)mc^2), & \text{multiphoton.} \end{cases} \tag{5}$$

Here, c is the speed of light *in vacuo*, $\gamma=(1+u^2)^{1/2}$ is the relativistic factor, $\mathbf{u}=\mathbf{p}/mc$, and $\mathbf{p}$ is the momentum variable. The relativistic formulation presented here permits treatment of cases where the laser is sufficiently intense to induce quiver velocities approaching c.

It is assumed that the laser pulse propagates along the z direction. Effecting the change of variables $z,t\rightarrow z,\tau=t-z/c$, the transport equation takes the form $df/d\tau=S/(1-\beta_z)$, where $\beta_z=c^{-1}dz/dt$. The transport equation can then be integrated along the characteristics, leading to

$$f(\mathbf{u},\tau)=n_n\int_{-\infty}^{\tau}\frac{d\tau'}{1-\beta_z(\tau')}\begin{cases} W_{tun}[E(\tau')]\delta(u(\tau')), & \text{tunneling}\\ W_{MPI}[E(\tau')]\delta(l\hbar\omega-U_i-[\gamma(\tau')-1]mc^2), & \text{multiphoton.}\end{cases} \tag{6}$$

Here, orbit $\mathbf{u}(\tau')$, $\gamma(\tau')$ [and the electric field $E(\tau')$] are all parametrized in terms of the time variable τ', with the requirement that the electron winds up at the phase space point $\mathbf{u}$, γ at time τ; i.e., $\mathbf{u}(\tau')|_{\tau'=\tau}=\mathbf{u}$, $\gamma(\tau')|_{\tau'=\tau}=\gamma$.

D. Laser field and equations of motion

The electric field and the vector potential $\mathbf{A}$ are related by $\mathbf{E}=-c^{-1}\partial\mathbf{A}/\partial t$. The normalized vector potential $\mathbf{a}=|e|\mathbf{A}/mc^2$ associated with the moving laser pulse is assumed to be given by the fundamental Gaussian [16]

$$\mathbf{a}=-\frac{a_0(\tau)}{2i}\exp(-i\omega\tau+i\theta)\exp(-r^2/w^2)\mathbf{e}_x+\text{c.c.}, \tag{7}$$

where $a_0(\tau)=\hat{a}_0\exp[-(\tau-\tau_0)^2/\tau_p^2]$ is the amplitude of the normalized vector potential, θ is a real-valued phase, w is the laser spot size, τ_0 is the centroid of the pulse, τ_p is the pulse duration and $\mathbf{e}_x$ is a unit vector along the x axis. In the following, it is assumed that the motion of electrons in the laser field can be described by the relativistically correct, classical equations; i.e.,

$$\frac{d\mathbf{p}}{dt}=-|e|\mathbf{E}-\frac{|e|}{\gamma mc}\mathbf{p}\times\mathbf{B},$$

where $\mathbf{B}$ is the magnetic field. In the paraxial approximation $\mathbf{B}\approx\mathbf{e}_z\times\mathbf{E}$, where $\mathbf{e}_z$ is a unit vector along the z axis.

The laser field given in Eq. (7) is peaked along the z axis. Electrons that are born in the high-intensity region are subject to a relatively slow radial ponderomotive drift towards the skirt of the laser beam. This slow drift can be analyzed by combining the equations of motion to obtain [17,18]

$$\frac{d\gamma_s^2}{dt}=\frac{\partial\langle\mathbf{a}^2\rangle}{\partial t}, \tag{8}$$

where γ_s is the slowly varying part of the relativistic factor and $\langle\cdots\rangle$ denotes a temporal average. An estimate of the time taken by an electron to radially drift across a beam waist w may be obtained by inserting Eq. (7) into Eq. (8). Neglecting diffraction and assuming the laser pulse is relatively long, it follows that if

$$\tau_p\ll\frac{w}{ca_0}, \tag{9}$$

the radial displacement of an electron as the laser pulse propagates through is negligible compared to w and one can consider the laser field to be nearly planar. Henceforth it is assumed that

$$\mathbf{a}=-a_0(\tau)\sin\omega\tau\mathbf{e}_x, \tag{10}$$

$$\mathbf{E}=|e|^{-1}mc\omega a_0(\tau)\cos\omega\tau\mathbf{e}_x. \tag{11}$$

For plane waves, the equations of motion combine into

$$\frac{d}{d\tau}(\mathbf{u}-\mathbf{a}-\gamma\mathbf{e}_z)=\mathbf{0}. \tag{12}$$

Equation (12) can be integrated to

$$\mathbf{u}_\perp(\tau')-\mathbf{a}_\perp(\tau')=\mathbf{u}_\perp(\tau)-\mathbf{a}_\perp(\tau)=\text{const}, \tag{13}$$

$$u_z(\tau')-\gamma(\tau')=u_z(\tau)-\gamma(\tau)=\text{const}, \tag{14}$$

where $a_z=E_z=0$ in the paraxial approximation and the suffix $\perp$ denotes the component that is transverse to the z axis.

Making use of the properties of the δ function, Eq. (6) simplifies to

$$f(u_x,u_z,\tau)=n_n\frac{mc}{|e|}\sum_i\frac{1}{E(\tau_i)}\begin{cases} W_{tun}[E(\tau_i)], & \text{tunneling,}\\ \dfrac{W_{MPI}[E(\tau_i)]\gamma(\tau_i)}{mc^2u_x(\tau_i)}, & \text{multiphoton.}\end{cases} \tag{15}$$

In Eq. (15) τ_i denotes an instant at which the δ function in Eq. (6) triggers and the summation is over all indices i such that $\tau_i \leqslant \tau$. These instants are determined from Eqs. (13) and (14). In particular, for tunneling ionization $u_x(\tau_i)=0$ and

$$a_x(\tau_i)=a_x(\tau)-u_x(\tau) \tag{16}$$

is an implicit equation for τ_i.

Making use of the definition of γ and Eq. (16), it follows that, for tunneling ionization,

$$u_z(\tau)=\gamma(\tau)-1. \tag{17}$$

It must be stressed that this relationship is a consequence of the "initial" condition that electrons are born at rest in the tunneling regime. Observe that Eq. (17) implies that all electrons have a forward-directed axial velocity. Making use of the definition of γ again, Eq. (17) can be rewritten as

$$\frac{u_x}{u_z}=\pm\sqrt{\frac{2}{\gamma-1}}. \tag{18}$$

This relationship [19,20] implies that the electron distribution can be expressed as a function of u_x only (as well as of τ).

For MPI, on the other hand, the electrons are born on a circle in the u_x-u_z plane. Specifically,

$$\gamma(\tau_i)\equiv\sqrt{1+[u_x(\tau_i)]^2+[u_z(\tau_i)]^2}=1+(l\hbar\omega-U_i)/mc^2. \tag{19}$$

The appropriate implicit equation for τ_i in this regime is

$$u_x(\tau_i)-a_x(\tau_i)=u_x(\tau)-a_x(\tau). \tag{20}$$

III. EXAMPLES

In this section examples of the distribution function are displayed to show the qualitatively different characteristics associated with tunneling ionization and multiphoton ionization. The plots are obtained numerically by performing the summation indicated in the analytical form for the distribution function. The radiation is linearly polarized, with $\lambda=1.06\ \mu$m, corresponding to the wavelength of Nd^{3+}:glass laser. With reasonable choices for the spot size w and the pulse length τ_p the constraint in Eq. (9) is readily satisfied. Moreover, the Rayleigh range Z_R can be made long enough that diffraction of the laser beam is negligible.

A. Tunneling ionization

An approximation to the form of the distribution function in the tunneling regime may be obtained as follows. Neglecting diffraction, Eq. (16) can be rewritten as

$$\sin\omega\tau_i=\frac{a_0(\tau)\sin\omega\tau+u_x}{a_0(\tau)}. \tag{21}$$

This equation is to be solved for τ_i that are to be inserted in Eq. (15). Since W_{tun} is a very sharply peaked function of the electric field, the dominant contribution to the sum in Eq. (15) is from those τ_i such that $\sin\omega\tau_i\approx 0$; i.e., the distribution function is peaked at

$$u_{tun,peak}(\tau)=-a_0(\tau)\sin\omega\tau. \tag{22}$$

Expanding $\cos\omega\tau_i$ about $\omega\tau_i=m\pi$, where m is an integer, it follows that

$$f_{tun}(u_x,\tau)\sim\exp\left\{-g\left[\frac{u_x-u_{tun,peak}}{a_0(\tau)}\right]^2\right\}, \tag{23}$$

where $g=[|e|/3mc\omega a_0(\tau)](U_i/U_H)^{3/2}(4\pi I_H/c)^{1/2}$. The tunneling ionization distribution function thus has the form of a Gaussian in the momentum variable u_x. The centroid of the Gaussian, given by Eq. (22), oscillates in time with frequency ω, with an excursion amplitude equal to $a_0(\tau)$. Superimposed on this, the Gaussian has a width that is proportional to three-quarters power of laser intensity $[\propto a_0^{3/2}(\tau)]$.

For the example in the tunneling ionization regime the gas consists of hydrogen atoms with ionization energy 13.6 eV. The peak laser intensity (averaged over the period) is $I_0=1$ PW/cm^2 with Keldysh parameter $\gamma_K=0.254$ and normalized laser vector potential $\hat{a}_0=0.029$. Before discussing the distribution function, it is interesting to examine the momentum-space relationship embodied by Eq. (18). This is done by performing a two-dimensional particle-in-cell simulation of a laser pulse propagating into an initially neutral gas of hydrogen. The intensity plots in Fig. 2 show the results, where each point represents an electron, placed according to its momentum variables at a particular instant in time. To start with the simplest case, the plot in Fig. 2(a) is for a plane wave, relatively early in time while all electrons are still in the laser pulse. Coordinates of points lying on the curve in this plot are found to be in good agreement with Eq. (18). Figure 2(b) shows the momentum-space plot a little later on, when electrons have slipped behind the laser pulse. As expected, the realistic case of a laser pulse with a finite (transverse) spot size is more complicated. Figure 2(c) shows the example of a laser beam with a spot size radius equal to 10 optical wavelengths. As ionization proceeds and plasma forms, the electron density approaches 0.1% of the critical density in the simulations shown in Figs. 2(b) and 2(c). The space charge field due to the plasma has the effect of smearing the energy-angle relationship of Eq. (18). For simulations in which the electron density does not build up significantly, the energy-angle relationship in Eq. (18) is found to hold extremely well.

Figure 3 is a surface plot of the electron distribution function in the tunneling regime, obtained from Eq. (15). The distribution function $f(u_x,\tau)$ is plotted along the vertical axis. One of the horizontal axes is u_x, while the other corresponds to $T\equiv\omega\tau/\pi$. The distribution function is plotted over roughly one period of oscillation, near the peak laser intensity. Oscillations of the centroid of the distribution function, as well as its Gaussian-like falloff with u_x are consistent with the prediction of Eq. (23). The ponderomotive energy U_p of the quivering electrons in this example is 104 eV. If the distribution function $F(E)$ is plotted as a function of

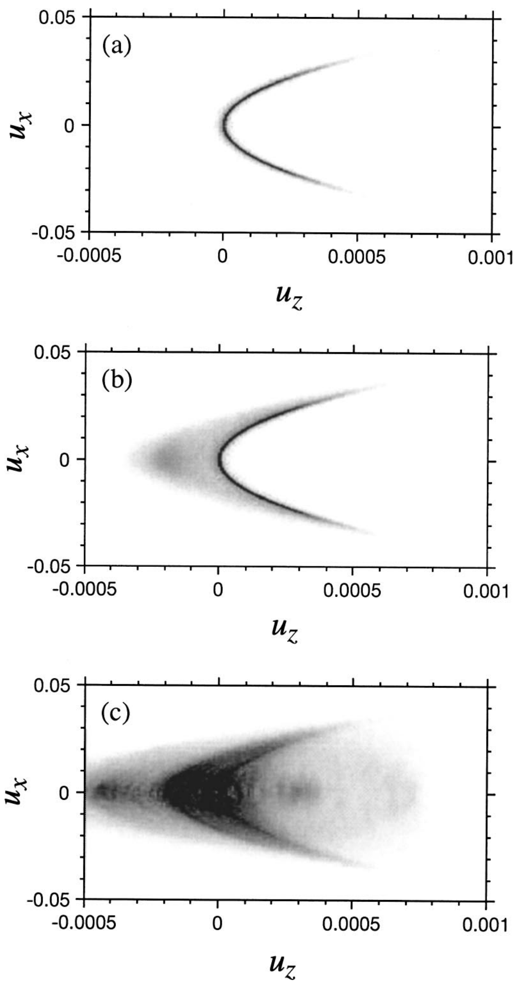

FIG. 2. Momentum-space plots in tunneling ionization. The intensity plot in (a) is for a plane wave, early on while electrons are in the pulse, whereas in (b) the electrons have slipped behind the pulse. The intensity plot in (c) is for laser beam with a spot size radius equal to 10 optical wavelengths.

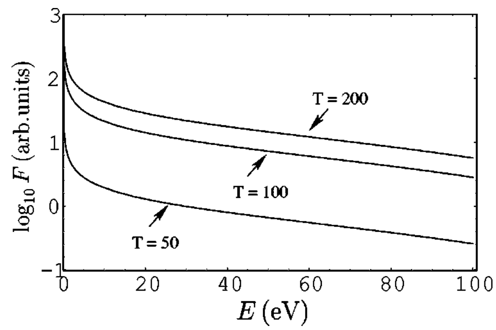

FIG. 4. Electron distribution function (in arbitrary units) in the tunneling regime plotted as a function of electron kinetic energy E. The three curves correspond to time instants $T\equiv\omega\tau/\pi=50$, 100, and 200.

electron kinetic energy, $E\equiv(\gamma-1)mc^2$, the plot in Fig. 4 is obtained. In Fig. 4, F is plotted at three different instants in time, labeled by $T=50$, 100, and 200. As time advances, the distribution function increases over the entire energy range as more and more electrons are released. Observe that—as indicated in Ref. [8]—for a linearly polarized laser beam the energy distribution function F peaks at small energies.

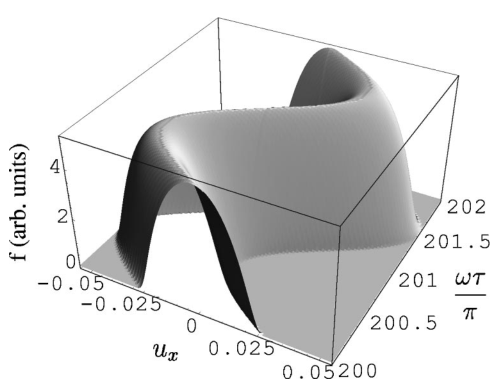

FIG. 3. Surface plot of electron distribution function $f(u_x,\tau)$ (in arbitrary units) in the tunneling regime.

B. Multiphoton ionization

Noting that for multiphoton ionization $\gamma(\tau_i)$ and $u_x(\tau_i)$ are constants for all i, the distribution function simplifies to

$$f_{MPI}(u_x,u_z,\tau)=n_n\frac{2\pi\omega/I_{MPI}^l}{(l-1)!}\frac{\gamma(\tau_i)}{|e|c\sqrt{(u_z-u_l)(u_r-u_z)}}\times\sum_i|E_0\cos\omega\tau_i|^{2l-1}, \quad (24)$$

where $\gamma(\tau_i)$ is the constant defined by Eq. (19). In writing Eq. (24), $u_x(\tau_i)$ in the denominator of Eq. (15) has been factorized as $\pm[(u_z-u_l)(u_r-u_z)]^{1/2}$, where

$$u_{l,r}=\frac{\gamma(\tau_i)u_x^2\mp\sqrt{[\gamma^2(\tau_i)-1]}(u_x^2+2)}{2}, \quad (25)$$

and the $-$ and $+$ in Eq. (25) correspond to the suffices l and r, respectively.

Examination of Eq. (24) reveals that f has singularities along curves $u_z=u_l$ and $u_z=u_r$ in momentum space. However, these are square-root singularities that are integrable and physically meaningful quantities such as the electron density $[\propto\int\int du_x du_z f(u_x,u_z,\tau)]$ are well behaved. These singularities originate from the u_x variable in the denominator of Eq. (15). Physically, therefore, the singularities are simply a reflection of the time interval that an electron spends in a given region of phase space as it executes quiver motion along the x axis.

Equation (24) may be used to obtain an approximate form for the distribution function. Neglecting diffraction, Eq. (20) can be rewritten as

$$\sin\omega\tau_i=\frac{a_0(\tau)\sin\omega\tau+u_x\mp[(u_z-u_l)(u_r-u_z)]^{1/2}}{a_0(\tau)}. \quad (26)$$

In Eq. (26) the upper (lower) sign is to be used according as u_x is positive (negative). The dominant contribution to the sum in Eq. (24) for large l is from τ_i that satisfy $\sin\omega\tau_i \approx 0$; i.e., the distribution function is peaked at

$$u_{MPI,peak}(u_x,u_z,\tau) = -a_0(\tau)\sin\omega\tau \pm[(u_z-u_l)(u_r-u_z)]^{1/2}. \quad (27)$$

Expanding $\cos\omega\tau_i$ about $\omega\tau_i = m\pi$, where m is an integer, it follows that

$$f_{MPI}(u_x,u_z,\tau) \sim \frac{1-l[u_x-u_{MPI,peak}(u_x,u_z,\tau)]^2/a_0^2(\tau)}{[(u_z-u_l)(u_r-u_z)]^{1/2}}. \quad (28)$$

Observe that since $u_{MPI,peak}$ is a function of u_x, the distribution in Eq. (28) does not have a simple parabolic variation with u_x. However, the centroid of the distribution, given by Eq. (27), oscillates in time with frequency ω and with an excursion amplitude equal to $a_0(\tau)$.

For the example in the multiphoton ionization regime, laser propagation in a medium with ionization energy equal to 11.7 eV is considered and the MPI cross section is taken to be $\sigma_{MPI} = 6.4\times10^{-18}$ cm^2 [21,22]. [These parameters are nearly those of the molecule O_2 (ionization energy being 12.1 eV); the surface plot for the distribution function is far better resolved for the lower ionization energy chosen.] The peak laser intensity (averaged over the period) is $I_0 = 50$ TW/cm^2, with Keldysh parameter $\gamma_K = 1.05$, and normalized laser vector potential $\hat{a}_0 = 0.0064$. The electron distribution function at $\tau-\tau_0 = 2.75\tau_p$, obtained from Eq. (24), is shown in Fig. 5. This plot corresponds to the minimum number of photons required for ionization of the molecule with 1.06 μm radiation; i.e., $l = l_0 = 10$. Following Eq. (28), it is noted that the distribution oscillates in time at optical frequency ω. For the plot in Fig. 5, an instant in time is picked such that the circular base of the distribution is centered on $u_x = u_z = 0$. (For improved presentation and clarity, the plot range for u_x is larger than that of u_z; hence the elliptical appearance of the base.) The ponderomotive energy U_p of the quivering electrons in this example is 5.2 eV. Following Eq. (24), it is remarked that there are two integrable singularities due to the zeros of the square root in the denominator. The rise in f with increasing $|u_z|$ is due to this. Although not shown here, for larger values of l, the circular base of the plot in Fig. 5 expands, in quantitative agreement with the prediction of Eq. (19). While electrons are all born on the circle given by Eq. (19) (assuming an infinitely long laser pulse), the quiver motion along the x axis leads to the observed width of f in the u_x direction. When plotted as a function of kinetic energy, plots similar to that in Fig. 5 lead to a series of relatively narrow peaks of decreasing value as l increases. The plot in Fig. 5 is consistent with the distribution in Eq. (28) in the region surrounding the peak at $u_{MPI,peak}$.

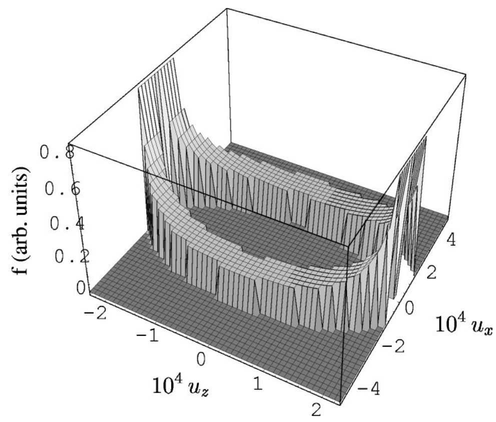

FIG. 5. Electron distribution function in multiphoton regime. The distribution (in arbitrary units) is plotted for 10 photon ionization, where $l_0 \equiv 10$ is the minimum number of photons required for ionization of the molecule with 1.06 μm radiation. The plot shows the distribution at an instant in time such that the circular base of the distribution function is centered on $u_x = u_z = 0$. For improved presentation and clarity, the plot range for u_x is larger than that of u_z, hence the elliptical appearance of the base.

IV. CONCLUSIONS

The electron distribution function is obtained in two limiting regimes of photoionization when a laser beam interacts with a gas. The two limits correspond to the tunneling and the multiphoton regimes. The transport equation for the distribution function is integrated along the characteristics defined by the classical equations of motion in the laser field. Analytical expressions for the distribution function have been obtained. Illustrative plots of the distribution function are presented and discussed. Two-dimensional particle-in-cell simulation results are also presented to demonstrate an interesting momentum-space pattern that is characteristic of tunneling ionization.

ACKNOWLEDGMENTS

This work was supported by the Office of Naval Research, the Joint Technology Office in support of the Navy DEW Program Office. A portion of this work was also supported by the U.S. Department of Energy Small Business Innovation Research (SBIR) grant to Icarus Research, Inc.

[1] Y.B. Zeldovich and Y.P. Raizer, *Physics of Shock Waves and High-Temperature Hydrodynamic Phenomena* (Academic, San Diego, 1966).
[2] Y.P. Raizer, *Laser-Induced Discharge Phenomena* (Consultants Bureau, New York, 1977).
[3] C.K. Rhodes, Science (Washington, DC, U.S.) **229**, 1345 (1985).
[4] N.B. Delone and V.P. Kraǐnov, *Multiphoton Processes in Atoms* (Springer, Berlin, 2000).
[5] T. Brabec and F. Krausz, Rev. Mod. Phys. **72**, 545 (2000).

[6] P. Agostini, F. Fabre, G. Mainfray, G. Petite, and N. Rahman, Phys. Rev. Lett. **42**, 1127 (1979).

[7] R.R. Freeman, P.H. Bucksbaum, H. Milchberg, S. Darack, D. Schumacher, and M.E. Geusic, Phys. Rev. Lett. **59**, 1092 (1987).

[8] P.B. Corkum, N.H. Burnett, and F. Brunel, Phys. Rev. Lett. **62**, 1259 (1989).

[9] M. Hentschel, R. Kienberger, C. Spielmann, G.A. Reider, N. Milosevic, T. Brabec, P. Corkum, U. Heinzmann, M. Drescher, and F. Krausz, Nature (London) **414**, 509 (2001).

[10] J. Itatani, F. Quéré, G.L. Yudin, M.Y. Ivanov, F. Krausz, and P.B. Corkum, Phys. Rev. Lett. **88**, 173903 (2002).

[11] L.V. Keldysh, Zh. Eksp. Teor. Fiz. **47**, 1945 (1964) [Sov. Phys. JETP **20**, 1307 (1965)].

[12] M.V. Ammosov, N.B. Delone, and V.P. Kraĭnov, Xh. Eksp. Teor. Fiz. **91**, 2008 (1986) [Sov. Phys. JETP **64**, 1191 (1986)].

[13] P. Pulsifer, J.P. Apruzese, J. Davis, and P. Kepple, Phys. Rev. A **49**, 3958 (1994).

[14] S. Augst, D. Strickland, D.D. Meyerhofer, S.L. Chin, and J.H. Eberly, Phys. Rev. Lett. **63**, 2212 (1989).

[15] M. Blaha and J. Davis, Phys. Rev. A **51**, 2308 (1995).

[16] P.W. Milonni and J.H. Eberly, *Lasers* (Wiley, New York, 1988).

[17] P. Sprangle, E. Esarey, J. Krall, and A. Ting, Opt. Commun. **124**, 69 (1996).

[18] B. Hafizi, A. Ting, E. Esarey, P. Sprangle, and J. Krall, Phys. Rev. E **55**, 5924 (1997).

[19] C.I. Moore, A. Ting, S.J. McNaught, J. Qiu, H.R. Burris, and P. Sprangle, Phys. Rev. Lett. **82**, 1688 (1999).

[20] C.I. Moore, A. Ting, T. Jones, E. Briscoe, B. Hafizi, R.F. Hubbard, and P. Sprangle, Phys. Plasmas **8**, 2481 (2001).

[21] A. Talebpour, J. Yang, and S.L. Chin, Opt. Commun. **163**, 29 (1999).

[22] J. Kasparian, R. Sauerbrey, and S.L. Chin, Appl. Phys. B: Lasers Opt. **71**, 877 (2000).